AMERICAN SOCIETY FOR MICROBIOLOGY | Antimicrobial Agents and Chemotherapy

Characterization of 22 Antituberculosis Drugs for Inhibitory Interaction Potential on Organic Anionic Transporter Polypeptide (OATP)-Mediated Uptake

M. Masud Parvez,[a] Jin Ah Jung,[b] Ho Jung Shin,[a] Dong Hyun Kim,[a] Jae-Gook Shin[a,b]

Department of Pharmacology, PharmacoGenomics Research Center (PGRC), Inje University College of Medicine, Busan, Republic of Korea[a]; Department of Clinical Pharmacology, Inje University Busan Paik Hospital, Busan, Republic of Korea[b]

We investigated the inhibitory interaction potential of 22 currently marketed antituberculosis (TB) drugs on organic anion-transporting polypeptide 1B1 (OATP1B1)-, OATP2B1-, and OATP1B3-mediated uptake using *in vitro Xenopus* oocytes and HEK cells. Rifabutin, ethambutol, amoxicillin, linezolid, *p*-amino salicylic acid, and rifapentine exhibited mild to moderate inhibitory effects on OATP-mediated uptake of estrone-3 sulfate, estradiol 17β-D-glucuronide, and rosuvastatin. The 50% inhibitory concentration (IC_{50}) values of rifabutin, amoxicillin, ethambutol, *p*-amino salicylic acid, and linezolid were 35.4, 36.2, 57.6, 72.6, and 65.9 μM, respectively, for uptake mediated by organic anionic transporter polypeptide 1B1 (OATP1B1) and 28.8, 28.9, 53.9, 31.5, and 61.0 μM, respectively, for uptake mediated by organic anionic transporter polypeptide 1B3 (OATP1B3). Streptomycin and linezolid showed greater inhibition of organic anionic transporter polypeptide 2B1 (OATP2B1)-mediated uptake, with IC_{50} values of 33.2 and 35.6 μM, respectively, along with mild inhibition of other drugs. Furthermore, rifabutin, amoxicillin, and rifapentine significantly inhibited OATP1B1-mediated rosuvastatin uptake, with IC_{50} values of 12.3, 13.0, and 11.0 μM, respectively, which showed a similar profile to estrone-3 sulfate uptake. The calculated *R* values ($[I]_{u\ inlet,max}/K_i$, where $[I]_{u\ inlet,max}$ represents the maximum estimated inhibitor concentration inlet to the liver and K_i is the inhibition constant) as the drug-drug interaction (DDI) indexes of PAS, ethambutol, and amoxicillin were 26.1, 6.5, and 4.3 for OATP1B1 and 52.0, 8.0, and 4.6 for OATP1B3, and those for streptomycin, amikacin, and linezolid were 5.0, 4.2, and 4.4 for OATP2B1, respectively, suggesting a higher possibility of *in vivo* DDIs. This study is the first comprehensive report to show the novel inhibitory potential of 22 marketed anti-TB drugs on OATP-mediated uptake, providing evidence for future *in vivo* clinical DDI studies.

Membrane transporters mediate the uptake and efflux of a broad variety of drugs and drug metabolites (1). Uptake transporters primarily belong to the solute carrier (SLC) superfamily. The expression patterns of transporters differ among tissues, such as the small intestine, liver, and kidneys (2). Inhibition or induction of organic anion-transporting polypeptide (OATP) transporter uptake plays a key role in the drug's pharmacokinetics, resulting in potential adverse effects (3). Thus, the role of transporters can be significantly associated with clinical phenotypes (4, 5). Translocation of one drug compound by a second drug is a major cause of drug-drug interactions (DDIs). Such translocations can occur with the inhibition of OATP transporters which can greatly affect the pharmacokinetics of a wide range of clinically used drugs (6). Hepatic uptake of drugs is facilitated by solute carrier (SLC) family transporters. To date, approximately 400 human SLC transporter genes have been reported within the SLC superfamily and classified into 46 subfamilies (7). Among the members of the superfamily, the OATP subfamily plays a major role in drug disposition in hepatocytes (8). In the liver, OATP transporters play a key role in DDIs due to expression and substrate specificity and function. Drugs that affect OATPs as inhibitors can also act as inducers of cytochrome enzymes but may or may not cause DDIs.

The World Health Organization (WHO) has recommended four first-line antituberculosis (anti-TB) drugs, isoniazid, rifampin, ethambutol, and pyrazinamide, as initial therapies for TB. Ten percent of TB patients have also been diagnosed with diabetes, and among the 9 million TB patients diagnosed in 2011, 13% were found to be coinfected with HIV (9). Due to multidrug regimen and unwanted pharmacokinetic/pharmacodynamic (PK/PD) effects, several DDIs and PK/PD effects have been reported in the literature, with case reports describing adverse events, nephrotoxicity, drug-induced liver injury (DILI), gastrointestinal (GI) disruption, serotogenicity, ocular toxicity, and neurotoxicity associated with INH, LZD, RIF, and EMB use during anti-TB therapy (9–12). A clinical DDI has also been reported to have taken place between theophylline and erythromycin via the OAT2 transporter (13). Rifampin is a first-line drug of choice to treat TB and has strong inhibitory potential against OATP-mediated uptake, which is likely to result in clinical DDIs (14). Rifampin also a substrate of the OATP1B1 (15) and OATP1B3 (16) membrane transporters, and several DDI studies have assessed and reported that competitive inhibition of OATP1B1/1B3 by rifampin may lead to reduced hepatic uptake of substrates. Studies on hepatic uptake of OATP1B1-mediated drugs have resulted in a list of sev-

Received 22 November 2015 **Returned for modification** 24 December 2015
Accepted 6 March 2016

Accepted manuscript posted online 14 March 2016

Citation Parvez MM, Jung JA, Shin HJ, Kim DH, Shin J-G. 2016. Characterization of 22 antituberculosis drugs for inhibitory interaction potential on organic anionic transporter polypeptide (OATP)-mediated uptake. Antimicrob Agents Chemother 60:3096–3105. doi:10.1128/AAC.02765-15.

Address correspondence to Jae-Gook Shin, phshinjg@inje.ac.kr.

Supplemental material for this article may be found at http://dx.doi.org/10.1128/AAC.02765-15.

eral compounds considered to be of clinical importance. The inhibitory effect of rifampin against OATP1B1-mediated uptake of the statin substrate pitavastatin was observed, and DDI prediction was based on *in vitro* data extrapolation using a static modeling approach (17).

Several statin drugs are known substrates of OATP2B1, including atorvastatin (18), rosuvastatin (19), and fluvastatin (20): these drugs can interact with other substrates, such as aliskiren (21), amiodarone (22), and glibenclamide (23), in the clinical setting and likely involve an interaction with OATP1B1 and/or OATP2B1 in the liver. The transporter-related study data can improve the patient safety and efficacy by selecting the optimum drug(s)/dose/regimen for patients who are taking medications known to be OATP substrates, such as statins or anti-HIV drugs. Data regarding transporter-mediated uptake/efflux inhibition by 22 marketed anti-TB drugs were not well characterized before: to address this issue, we conducted this study. We hypothesized that, not only rifampin, but other anti-TB drugs may have the potential to inhibit OATP transporter-mediated uptake which may cause DDIs. The aim of this study was to investigate the OATP1B1-, OATP2B1-, and OATP1B3-mediated uptake inhibitory effects and DDI potentials of 22 currently marketed anti-TB drugs using *Xenopus* oocytes and the HEK cell system. Significant inhibition was further characterized by kinetic investigations, which were further used to evaluate the *in vivo* DDI index (*R* value). The pharmacokinetic parameters of the inhibitors used to calculate *R* values are shown in Table S1 in the supplemental material (41–62). The results of this study may be helpful in designing personalized TB management regimens.

MATERIALS AND METHODS

Chemicals and reagents. [^{3}H]estrone-3-sulfate ([^{3}H]ES [2.12 TBq/mmol]) and [^{3}H]estradiol 17β-D-glucuronide ([^{3}H]E2G [1.27 TBq/mmol]) were purchased from PerkinElmer (Waltham, MA). All anti-TB drugs, isoniazid (INH), ethambutol (EMB), pyrazinamide (PZA), rifampin (RIF), rifabutin (RFB), amikacin (AMK), kanamycin (KAN), streptomycin (STR), moxifloxacin (MXF), ciprofloxacin (CIP), levofloxacin (LVX), cycloserine (CS), *p*-aminosalicylate acid (PAS), prothionamide (PRO), ethionamide (ETA), linezolid (LZD), amoxicillin (AMX), clarithromycin (CLR), roxithromycin (RXM), clofazimine (CFZ), bedaquiline (BQN), and rifapentine (RFP), were purchased from Sigma-Aldrich. Other reagents used in this study were purchased from commercial suppliers.

Generation of HEK293 cells stably expressing OATP1B1 and OATP2B1. HEK293 cells were grown in tissue culture flasks in Dulbecco's modified Eagle's medium (DMEM) supplemented with 10% fetal bovine serum (FBS), 1% nonessential amino acids, 2 mM L-glutamine, and 100 U/ml polysaccharide (PS). The pcDNA3.1-OATP1B1, pcDNA3.1-OATP2B1, and pcDNA3.1 plasmid vectors without inserts were transfected into HEK293 cells using Lipofectamine 2000 (Invitrogen) according to the manufacturer's protocol. At 24 h after the transfection, the cells were subcultured in medium containing 400 μg/ml Geneticin (Invitrogen). Cell clones were isolated using a cloning cylinder (24). Among the cell clones obtained, those showing the highest level of uptake for their specific-substrates were selected and designated HEK-OATP1B1 and HEK-OATP2B1. The OATP1B3 cDNA was transiently transfected into HEK293 cells using Lipofectamine 2000 (Invitrogen) according to the manufacturer's instructions.

Construction of HEK293 cells transiently transfected with OATP1B3 cDNA. HEK293 cells were maintained in a humidified atmosphere of 5% CO_2–95% air and grown in DMEM supplemented with 10% FBS, 2 mM L-glutamine, and 100 U/ml PS. The medium was changed every 2 days. After the culture had reached 90% confluence, the cells were trypsinized and24-well plates were seeded at a density of 2×10^5/well. At 90% confluence, the cell culture medium was replaced with serum-free medium 2 h before transfection. Transient transfection of pcDNA3.1 and pcDNA3.1-OATP1B3 into HEK293 cells was performed using Lipofectamine 2000. After transfection, the cells were incubated for 48 h at 37°C. Uptake studies were performed after the transfected cells formed a monolayer. The medium was removed from the HEK293 cell cultures, and the cells were washed with DMEM and preincubated for 1 h with serum-free DMEM at 37°C.

Cell culture. HEK-OATP1B1, HEK-OATP2B1, and HEK-OATP1B3 cells were grown in tissue culture flasks in DMEM supplemented with 10% FBS, 1% nonessential amino acids, 2 mM L-glutamine, and 100 U/ml PS at 37°C in 5% CO_2–95% air. The confluent cell layer was harvested using trypsin-EDTA, resuspended in culture medium, and replated. This process was repeated to obtain sufficient cells for the experiment.

[^{3}H]ES and [^{3}H]E2G cellular uptake studies: transport measurements using *Xenopus laevis* oocytes. For inhibition experiments, the probe substrate, TB drugs, and positive-control inhibitor were diluted in ND96 solution. Oocytes expressing OATP1B1, OATTP2B1, and OATP1B3 were incubated for 60 min in ND96 solution containing 45 nM [^{3}H]ES and 60 nM [^{3}H]E2G in the absence or presence of inhibitors. The incubation was terminated by adding ice-cold ND96 solution. After being washed five times, each oocyte was transferred to a scintillation vial and solubilized in 0.35 ml 10% SDS. After addition of scintillation fluid, the radioactivity in each oocyte was counted using a liquid scintillation counter.

Uptake of [^{3}H]ES and [^{3}H]E2G into HEK cells. We evaluated the cellular uptake of [^{3}H]ES and [^{3}H]E2G. Twenty-four-well culture plates were seeded with HEK-OATP1B1, HEK-OATP2B1, and HEK-OATP1B3 cells at a density of 2×10^5/well and incubated in an atmosphere of 5% CO_2–95% air at 37°C for 1 day. After the cells reached ~90% confluence, the cell monolayers were washed twice with phosphate-buffered saline (PBS) and preincubated for 20 min after replacing the medium with DMEM lacking FBS and PS. The cells were incubated in medium containing 45 nM [^{3}H]ES and 60 nM [^{3}H]E2G for 5 min at 37°C, after which the medium was aspirated immediately. The cell monolayers were washed three times with ice-cold PBS and solubilized in 1% Triton X-100 for 30 min at room temperature on a shaker. The amount of accumulated substrate within the cells was determined by measuring the radioactivity using a liquid scintillation counter (PerkinElmer).

[^{3}H]ES and [^{3}H]E2G uptake inhibition by anti-TB drugs. To evaluate the inhibitory effect of anti-TB drugs on the cellular uptake of [^{3}H]ES and [^{3}H]E2G, the HEK-OATP1B1, HEK-OATP2B1, and HEK-OATP1B3 cells were stably transfected. Rifampin (100 μM) for OATP1B1 and bromosulfophthalein (BSP [30 μM]) for OATP2B1 and OATP1B3 were used as positive-control inhibitors for uptake inhibition. The amount of substrate that accumulated within the cells was determined by measuring the radioactivity using liquid scintillation counting.

Effect of anti-TB drugs on rosuvastatin uptake by OATP1B1. To determine the inhibitory potential of anti-TB drugs, we used rosuvastatin as a sensitive substrate according to the FDA guideline for OATP1B1 drug interaction studies *in vitro*. We followed the same method described above, using rosuvastatin (1 μM) in the presence or absence of anti-TB drugs (100 μM). Aliquots (120 μl) of cell samples after rosuvastatin uptake were analyzed by liquid chromatography-tandem mass spectrometry (LC-MS/MS) to detect rosuvastatin uptake.

Sample preparation and LC-MS/MS analysis. Detection of rosuvastatin was performed as described previously (38). Briefly, after aspiration of the cellular uptake medium and being washed with ice-cold Dulbecco's phosphate-buffered saline (DPBS) three times, cells were solubilized in 0.1 M sodium hydroxide. The cells were collected by adding 100 μl acetonitrile (ACN [70%]) in a 1.5-ml tube, homogenized by sonication (3 to 5 s), and centrifuged (13,000 rpm, 10 min). The supernatant was recovered, and after addition of an internal standard (IS) compound for LC-

MS/MS and vortexing for 3 s, the solution was transferred to a LC-MS/MS vial for detection of rosuvastatin uptake into the cells.

Data analysis and kinetics of the uptake study. For the experiments, eight *Xenopus* oocytes and three wells of the cell system were used for each drug concentration. The values obtained in each experiment are expressed as means ± standard deviation (SD). To ensure that uptake inhibition only occurred with the selected transporters, we used mock cells as controls and a positive control for all experiments. Inhibition kinetics (50% inhibitory concentration [IC_{50}]) were determined using the inhibitory effect model, $E = E_0 \times \{1 - [C/(C + IC_{50})]\}$, where E_0 indicates inhibitory effect, E indicates the uptake of 9% of the control, and IC_{50} is the concentration for 50% inhibitory effect in Winnonlin (Parasight, version 5.1) and Sigmaplot 8.0 (SPSS, Inc., Chicago, IL).

Furthermore, we estimated the inhibition constant, K_i, with the equation $K_i = IC_{50}/1 + [S]/K_m$, which was established by Amundsen et al. (25), where K_m indicates the Michaelis-Menten constant of the substrate binding affinity for the transporter, and [S] indicates the substrate concentration in the incubation buffer used in the *in vitro* uptake inhibition experiment.

Prototype radioisotope substrate uptake was expressed as a volume, determined as the substrate amount associated with the cells (disintegrations per minute per well or picomoles per well) divided by the incubation concentration of the buffer (disintegrations per minute per milliliter or picomoles) and the amount of protein (milligrams of protein per well). The net uptake of OATP1B1, OATP2B1, and OATP1B3 was determined by subtracting the total amount of uptake in control cells from the uptake in OATP transporter-expressing cells. The kinetic parameter (concentration-dependent uptake) was evaluated by the Michaelis-Menten equation and followed a previously published method (26).

Drug-drug interaction index prediction using a static model. To relate our findings to clinical applications, we calculated the DDI index (26–28) according to the FDA guideline for OATP using total C_{max} and the unbound concentration (based on clinical data and label of the drugs) for each drug and K_i for the probe and rosuvastatin from our *in vitro* data, by plotting the equation mentioned in the FDA guideline and other reports (26, 29–31) to predict the possibility of a clinical DDI. There are several guidelines and specifications for DDI prediction from the FDA (draft version 2012), CDER (2012), the European Union (Committee for Human Medicinal Products, 2012), and Japan (Ministry of Health, Labor, and Welfare, 2014). The FDA recommends two steps for a decision-making tree to evaluate the inhibition of hepatic uptake transporters.

As a first step for calculating DDI for the inhibitory potential of any drug affecting substrate uptake by transporters, the R value was calculated as recommended by the FDA and others as $R = 1 + C_{max}/K_i$, where C_{max} indicates the maximum concentration of the inhibitor present in the systemic (bound + unbound) circulation. As a second step, the FDA, EMA, and MHLW recommend using the equation $R = 1 + [I]_{u\ inlet,max}/K_i$, where $[I]_{u\ inlet,max}$ indicates the maximum estimated inhibitor concentration inlet to the liver, as shown by the equation $[I]_{u\ inlet,max} = f_u \times [I_{max} + (K_a \times F_a \times F_g \times dose)/Q_h]$, where F_u is the unbound fraction of an inhibitor in the systemic circulation, calculated by assuming the blood-to-plasma (B/P) ratio, I_{max} is the maximum concentration of an inhibitor present in the blood, K_a is the absorption rate constant of the inhibitor, F_a is the absorbed fraction dose of the inhibitor, F_g is the fraction of the absorbed inhibitor dose from gut wall extraction, "dose" is the dose of the inhibitor, and Q_h is the hepatic blood flow rate (97 liters/h) (EU, Committee for Human Medicinal Products, 2012; Japan, Ministry of Health, Labor, and Welfare, 2014). We determined the R value using $K_a = 0.1$/min and $F_a \times F_g = 1$ to avoid the risk of false-negative DDI predictions in our study, as described previously (26).

Statistical analysis. We used a two-sided Student's t test to determine the statistical significance of differences between control and test data. Results are expressed as means ± SD. P values of <0.05 were considered to indicate a statistically significant difference from the control.

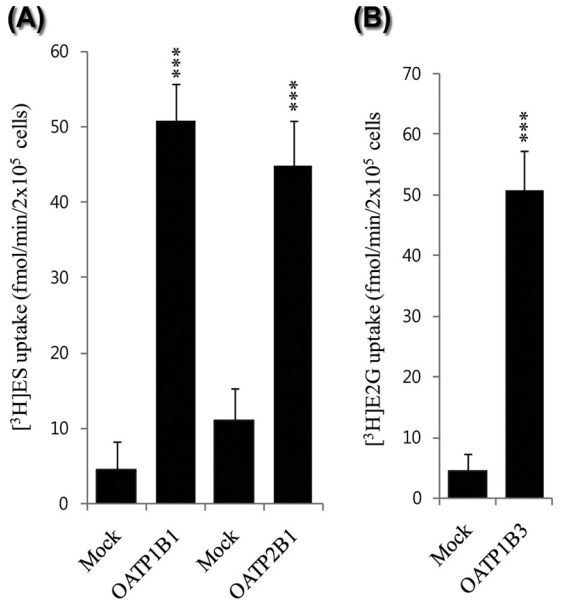

FIG 1 Uptake of (A) 45 nM [^{3}H]ES in human OATP1B1 (hOATP1B1)- and hOATP2B1-transfected HEK293 cells and (B) 60 nM [^{3}H]E2G uptake in hOATP1B3-transfected HEK293 cells. Mock-transfected [pcDNA3.1(+) transfection] HEK293 cells were used as the negative control. Data represent the means ± SD from three or more independent experiments ($n = 3$) *, $P < 0.05$, **, $P < 0.01$, and ***, $P < 0.001$, significantly different compared with percentage of uptake in controls.

RESULTS

Uptake of [^{3}H]ES and [^{3}H]E2G. Uptake values of [^{3}H]ES for OATP1B1 and OATP2B1 and [^{3}H]E2G for OATP1B3 were determined (Fig. 1) as a positive control (prototype substrate) in the experiments. In transporter-overexpressing *Xenopus* oocytes, we found the uptake values to be 23-, 12-, and 15-fold higher, respectively, than those of the control (see Fig. S1 in the supplemental material), and in the HEK-1B1-, HEK-2B1-, and HEK-1B3-overexpressing cells, the probe substrate uptake values were 10-, 9-, and 10-fold higher, respectively, than those of the control (mock) cells (Fig. 1). These results indicated that the cells were suitable for conducting uptake experiments. The uptake kinetics of the probe substrate indicated that the transfected HEK-OATP1B1, HEK-OATP2B1, and HEK-OATP1B3 cells were suitable for use in the uptake experiment (Table 1) using nonlinear kinetics, as described in Materials and Methods. We also assessed the time-dependent uptake of the probe substrate (data not shown) in transfected cells. We chose 5 min for the uptake experiments, as reported previously (31).

Effects of anti-TB drugs on OATP1B1-mediated [^{3}H]ES uptake. In the OATP1B1-overexpressing HEK293 cell uptake experiments, 100 μM RIF was used as a positive-control inhibitor, and it almost totally abolished [^{3}H]ES uptake, by 93%, compared with that of control cells (Fig. 2). Next, RFB, EMB, PAS, AMX, and RFP showed significant inhibition of [^{3}H]ES uptake by 87, 76, 70, 72, and 80%, respectively, compared with control uptake. INH, PZA, LZD, CLR, and BQN showed moderate inhibitory effects (40 to 65%), and PRO, ETA, and CFZ showed mild inhibition of [^{3}H]ES uptake (Fig. 2A); these results were similar to those for *Xenopus* oocytes (data not shown). From this inhibition screening, we estimated the inhibitory kinetics (IC_{50}) and K_i for the potent drugs

TABLE 1 Functional characterization of stably transfected HEK-OATP1B1 and HEK-OATP2B1 cells and transiently transfected HEK-OATP1B3 cells for uptake of radiolabeled *in vitro* probe substrates[a]

Substrate[b]	Transporter	K_m (μM)	V_{max} (pmol/min/mg protein)	CL_{int} (μl/min/mg protein)	Reported K_m (μM)[c]
[^{3}H]ES	OATP1B1	2.3	28.0	12.17	2.4 (37), 12.5 (38)
[^{3}H]ES	OATP2B1	5.8	32.0	6.4	7.1 (23), 8.09 (39), 10.2 (40)
[^{3}H]E2G	OATP1B3	8.4	12.0	1.52	15.8 (37), 24.6 (17)

[a] Shown are the intracellular uptake kinetics of the cells derived from *in vitro* experiments: K_m, Michelis-Menten constant; V_{max}, maximum rate of uptake; CL_{int}, intrinsic clearance per unit of time. Data represent the mean values from triplicate experiments.
[b] [^{3}H]estrone-3-sulfate ([^{3}H]ES) for OATP1B1 and OATP2B1 and [^{3}H]estradiol β-D-glucuronide ([^{3}H]E2G) for OATP1B3 with the substrate in a concentration range of 0.1 to 100 μM were normalized to the control and used to determine cell function.
[c] Reported K_m values represent previously published reference data from the references cited in parentheses.

at a concentration range of 1 to 200 μM. Furthermore, estrone sulfate, a prototype substrate for OATP1B1, was used at a lower concentration than its K_m value in the presence of the anti-TB drugs. The anti-TB drugs showed concentration-dependent inhibition of uptake (Fig. 3), and the estimated IC_{50} values for RFB, EMB, PAS, AMX, LZD, and RFP were 35.4, 57.6, 72.6, 36.2, 65.9, and 26.7 μM, respectively (Table 2).

Effects of anti-TB drugs on OATP2B1-mediated uptake. We also assessed whether the anti-TB drugs had inhibitory potential on OATP2B1-mediated uptake in *in vitro* experiments. In stably transfected cells, in an OATP2B1-mediated uptake study, 30 μM BSP was used as positive-control inhibitor, and it almost abolished [^{3}H]ES uptake, by 80%, compared with control cells. RFB, KAN, STR, LZD, AMX, and RFP showed signif-

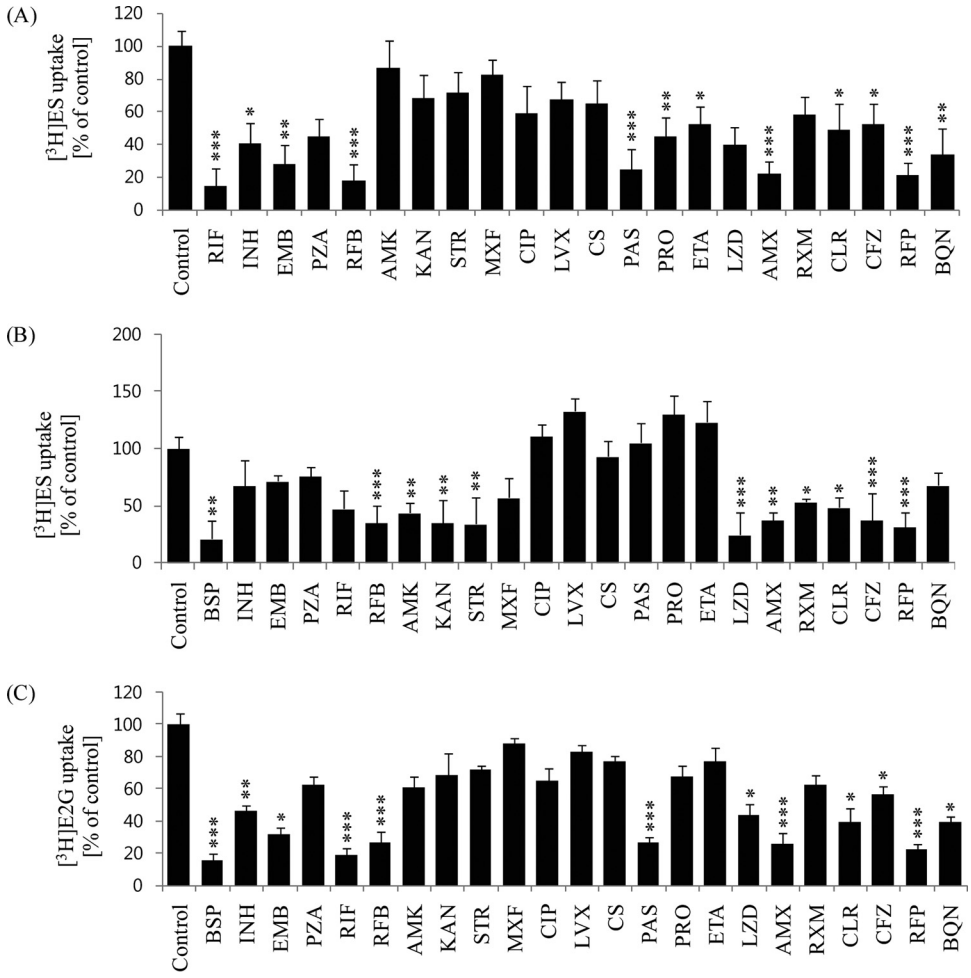

FIG 2 Screening of the inhibitory effects of 22 anti-TB drugs on uptake ability. (A) [^{3}H]ES (45 nM) in stably transfected HEK-OATP1B1 cells. (B) [^{3}H]ES (45 nM) in stably transfected HEK-OATP2B1 cells. (C) [^{3}H]E2G (60 nM) in transiently transfected HEK-OATP1B3 cells. In the absence of any inhibitors, OATP1B1-, OATP2B1-, and OATP1B3-mediated uptake, as a control, was compared with TB drug-mediated uptake inhibition. Rifampin for OATP1B1 and bromosulfophthalein (BSP) for OATP2B1 and OATP1B3 were used as positive controls for uptake inhibition. Data are presented as the mean ± SD value from three or more independent experiments. *, $P < 0.05$, **, $P < 0.01$, and ***, $P < 0.001$, significantly different compared with the percentage of uptake in the control (no inhibitor).

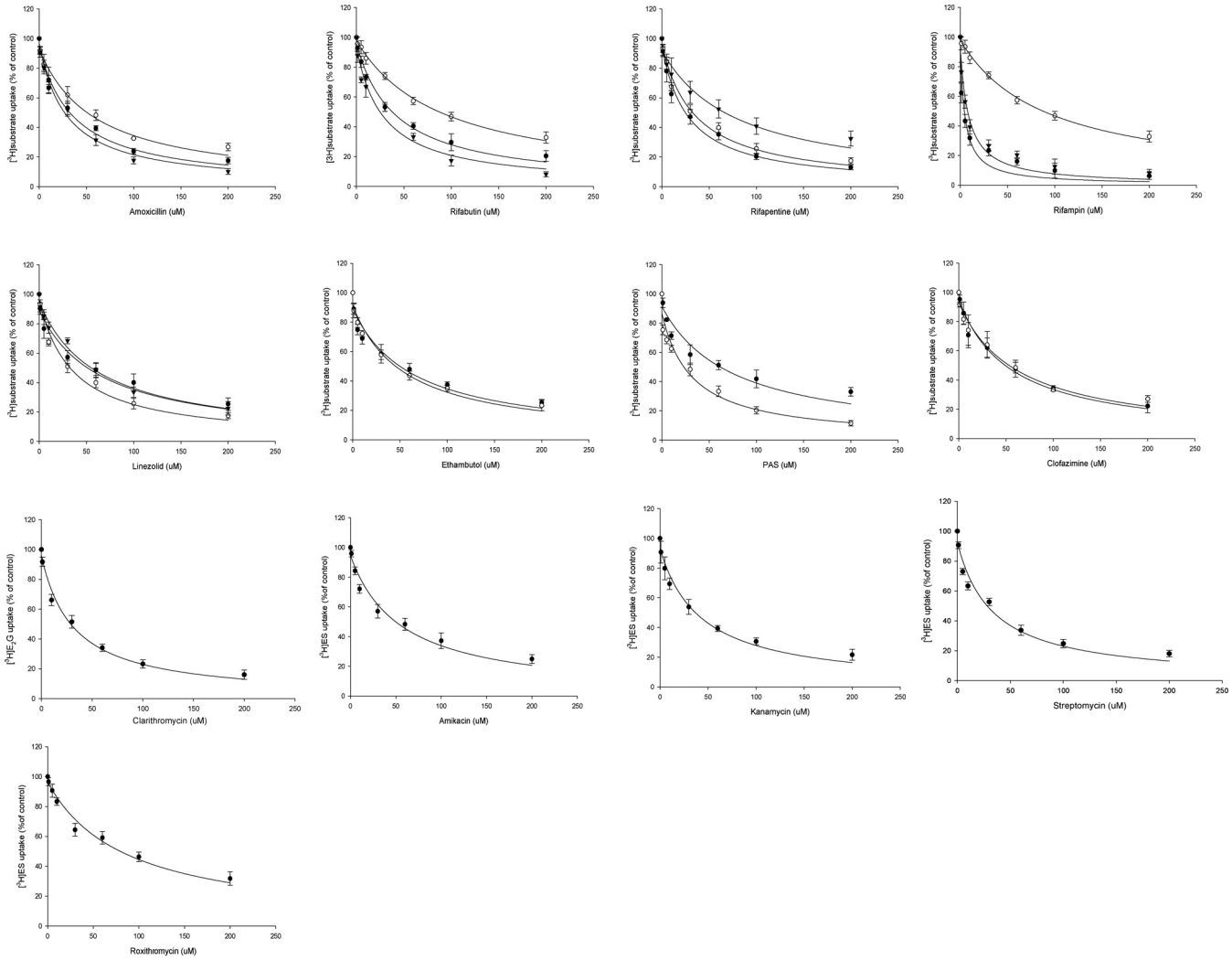

FIG 3 Estimation of the inhibitory kinetics of anti-TB drugs on 45 nM [^{3}H]ES and 60 nM [^{3}H]E2G uptake into transfected HEK cells. Inhibitory properties overlapped for those drugs as the three-line graphs represent OATP1B1 (○), OATP2B1 (●), and OATP1B3 (▼), two-line graphs represent OATP1B1 (●) and OATP1B3 (○), and a single-line graph represents clarithromycin for OATP1B3-mediated E2G and amikacin, kanamycin, streptomycin, and roxithromycin for OATP2B1-mediated ES uptake, respectively. The estimated IC_{50} was calculated by nonlinear kinetics using Winnonlin 6.0. Data are presented as the mean ± SD, relative to the control (no inhibitor), from three or more independent experiments.

icant inhibition, of 78, 73, 72, 80, 70, and 72%, respectively, on [^{3}H]ES uptake. RIF, AMK, RXM, and CLR showed moderate inhibitory effects (40 to 65%), and INH and BQN showed mild inhibition on [^{3}H]ES uptake (Fig. 2B). The estimated inhibition kinetics (IC_{50}) for OATP2B1 by LZD, AMX, KAN, STR, and RFP were 35.6, 56.6, 42.9, 33.2, and 36.1 μM, respectively (Table 2).

Effects of anti-TB drugs on OATP1B3-mediated uptake. Along with OATP1B1 and OATP2B1, we also evaluated OATP1B3 uptake inhibition of anti-TB drugs in transiently transfected HEK293 cells by incubation with 60 nM [^{3}H]E2G in the absence or presence of anti-TB drugs. The results showed that some anti-TB drugs had inhibitory potential on OATP1B3-mediated uptake (Fig. 2C). BSP was used as a positive-control inhibitor and showed over 84% inhibition of E2G uptake by OATP1B3. RFB, PAS, AMX, and RFP showed significant inhibition of E2G uptake of 76, 70, 69, and 82%, respectively, by OATP1B3-transfected cells compared with control cells. These results displayed a similar profile to the *Xenopus* oocytes (data not shown). The results showed that INH, LZD, CLR, and BQN had moderate (45 to 65%) inhibition of OATP1B3-mediated uptake, and the tested anti-TB drugs showed mild inhibitory potential. We thus estimated the inhibition kinetics on OATP1B3-mediated uptake of [^{3}H]E2G (Fig. 3), and the IC_{50} values for PAS, RFB, EMB, LZD, AMX, CLR, CFZ, and RFP were 31.2, 26.3, 53.2, 60.4, 28.6, 31.2, 58.2, and 70.3 μM, respectively (Table 2).

Effect of anti-TB drugs on rosuvastatin uptake by OATP1B1. We next evaluated the inhibitory effects of anti-TB drugs on rosuvastatin uptake in HEK-OATP1B1 cells. The inhibitory potential for some drugs was significant compared with that of the positive-control inhibitor, rifampin. Ethambutol, linezolid, PAS, amoxicillin, and rifabutin showed 80, 71, 73, 81, and 82% inhibition, respectively (Fig. 4). We selected those anti-TB drugs that revealed significant inhibitory properties on OATP1B1-mediated

TABLE 2 Summary of inhibitory kinetics (IC_{50}) of anti-TB drugs on hOATP1B1- and hOATP2B1-mediated uptake of [^{3}H]ES and hOATP1B3-mediated uptake of [^{3}H]E2G[a]

Anti-TB drug	IC_{50} (μM)		
	OATP1B1	OATP2B1	OATP1B3
PAS	72.6 ± 14.0	ND	31.5 ± 4.9
Rifabutin	35.4 ± 2.7	57.4 ± 9.4	28.8 ± 1.9
Ethambutol	57.6 ± 3.0	ND	53.9 ± 6.7
Linezolid	65.9 ± 15.9	35.6 ± 6.8	61.0 ± 7.7
Amoxicillin	36.2 ± 2.7	56.6 ± 5.1	28.9 ± 4.5
Clarithromycin	ND	ND	31.5 ± 4.22
Clofazimine	ND	56.7 ± 9.6	59.0 ± 4.8
Rifampin	1.9 ± 0.16	91.0 ± 14.6	6.4 ± 0.5
Amikacin	ND	55.4 ± 9.5	ND
Kanamycin	ND	42.9 ± 2.0	ND
Streptomycin	ND	33.2 ± 2.0	ND
Roxithromycin	ND	80.0 ± 5.3	ND
Rifapentine	26.7 ± 4.6	36.1 ± 3.5	71.0 ± 9.0

[a] The concentrations of the *in vitro* prototype substrates [^{3}H]ES and [^{3}H]E2G were 45 and 60 nM, respectively. The corresponding substrate for the transporter was incubated with anti-TB drugs in the concentration range of 1 to 200 μM. Data are presented as means ± SD from three or more independent experiments. The estimated IC_{50} was calculated by nonlinear kinetics as described in Materials and Methods by using Winnonlin 6.0. ND, not determined.

prototype substrate [^{3}H]ES uptake. The ethambutol, linezolid, PAS, amoxicillin, rifapentine, and rifabutin also showed concentration-dependent inhibition on rosuvastatin uptake (see Fig. S3 in the supplemental material).

Drug-drug interaction index prediction by the *R* value. We further evaluated the DDI index, as the *R* value, using a static model to assess the correlation of the outcomes for the anti-TB drugs having significant inhibitory potential. The *R* value for human OATP1B1 (hOATP1B1) showed that several anti-TB drugs have the potential to interact with the uptake of substrates. PAS, EMB, and AMX showed the highest DDI index *R* values for OATP1B1: 26.1, 6.52, and 4.33, respectively (Table 3). Similarly, the OATP1B1-mediated *R* value for rosuvastatin uptake inhibition is summarized separately (Table 4). The *R* value for OATP2B1 indicated DDI potential too (Table 3): LZD, AMX, AMK, and STR showed the highest *R* values, which were 4.43, 3.1, 4.21, and 5.00, respectively. Similarly, the *R* values for OATP1B3 of PAS, EMB, AMX, and CLR were 51.9, 8.0, 4.67, and 2.52 (Table 3), like the highest DDI index values, calculated with $[I] = [I]_{u\ inlet,max}$. We did not calculate *R* values (DDI index) for drugs that did not significantly inhibit OATP-mediated uptake in the screening and inhibition kinetic study.

DISCUSSION

This study revealed the inhibitory properties of anti-TB drugs on OATP-mediated uptake and their DDI potential. Several clinically used anti-TB drugs were found to inhibit OATP transport activity *in vitro* and clinical DDIs, many of which are not OATP substrates (30). It is noted that all substrates can competitively inhibit other substrates that bind to the same site on OATPs. Potent inhibitors showed 50% inhibitory concentration (IC_{50}) values that may be important for at least some substrates' disposition. One study showed that a single 600-mg intravenous dose of rifampin raised the mean AUC of atorvastatin by more than 600%, probably by inhibiting OATP1B1- and/or OATP1B3-mediated hepatic uptake of atorvastatin (29). Among 22 anti-TB drugs explored by the present study, PAS, AMX, EMB, and LZD showed the highest inhibition potential. In the case of OATP1B1-mediated uptake inhibition, PAS, AMX, LZD, and EMB showed high DDI indexes (*R* values), suggesting high DDI potential. Following the guidelines for prototypical substrates, the *R* values determined were greater than the corresponding cutoff values recommended by regulatory agencies for both C_{max} ($R \geq 1.1$, FDA) and $[I]_{u\ inlet,max}$ ($R \geq 1.25$, FDA and MHLW; $R \geq 1.04$, EMA) conditions, where the *R* value was expressed as the suggested value according to the upper limit of the equivalence range by the FDA. An inhibition potential (K_i) lower than the unbound C_{max} indicates those drugs have the potential to cause significant clinical DDIs according to the FDA. Among the drugs tested, PAS, EMB, and AMX for OATP1B1 (Fig. 2), LZD, AMX, AMK STR, for OATP2B1 (Fig. 2) and PAS, EMB, LZD, and AMX for OATP1B3 showed K_i values lower than the unbound C_{max}. However, RXM for OATP2B1 and CLR for OATP1B3 showed K_i values higher than the unbound C_{max}. Although the *R* value was higher than the marginal value for DDI prediction, according to FDA, EMA, and MHLW DDI prediction guidelines, this may imply that the drugs are not clinically effective due to a lower unbound concentration than the K_i (26–28). While the drug substrates of OATP1B3 overlap those of OATP1B1, OATP1B3 appears to be the only hepatic OATP that transports digoxin, docetaxel, and paclitaxel. In contrast to OATP1B1 and OATP2B1, OATP1B3 has also been identified to transport several substrates *in vitro*. In an example of a previously reported clinical DDI, the linezolid C_{max} increased almost 2-fold when coadministered with clarithromycin in MDR-TB patients. In this case, the possible DDI mechanism was proposed to be transporter mediated, although this has not been confirmed mechanistically (32). Another study in methicillin-resistant *Staphylococcus aureus* (MRSA) patients showed that rifampin caused a lower serum concentration of linezolid, possibly caused by the induction of P450 cytochromes (CYPs) (33).

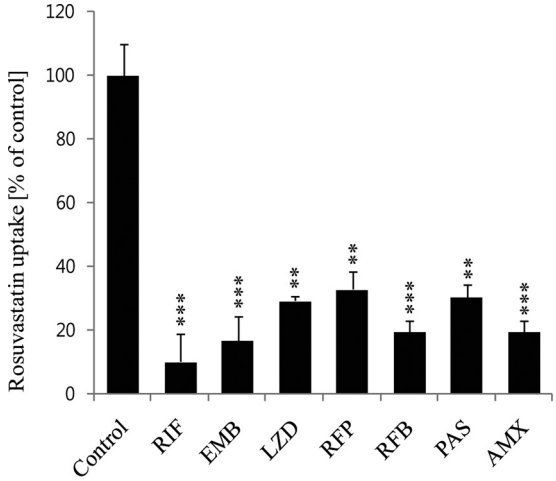

FIG 4 Inhibitory effects of anti-TB drugs on 1 μM rosuvastatin uptake in stably transfected HEK-OATP1B1 cells. OATP1B1-mediated (in the absence of any uptake inhibitor) uptake, as a control, was compared with uptake inhibition by the TB drugs. Rifampin (RIF) was used as a positive control for OATP1B3-mediated uptake inhibition. Data represent the means ± standard errors (SE) from triplicate experiments ($n = 3$). *, $P < 0.05$, **, $P < 0.01$, and ***, $P < 0.001$, significantly different compared with percentage of uptake in controls (no inhibitor).

TABLE 3 The drug-drug interaction index predicted from *in vitro* OATP1B1- and OATP2B1-mediated [^{3}H]ES and OATP1B3-mediated [^{3}H]E2G uptake inhibited by anti-TB drugs[a]

	DDI index (R value = 1 + $[I]/K_i$) for:					
	OATP1B1		OATP2B1		OATP1B3	
Anti-TB drug	$[I] = C_{max}$	$[I] = [I]_{u\ inlet,max}$	$[I] = C_{max}$	$[I] = [I]_{u\ inlet,max}$	$[I] = C_{max}$	$[I] = [I]_{u\ inlet,max}$
PAS	13.70 ± 2.3*	26.1 ± 4.7*	ND	ND	26.70 ± 2.7*	51.90 ± 5.4*
Rifabutin	1.02 ± 0.002	1.10 ± 0.008	1.13 ± 0.002	1.04 ± 0.05	1.02 ± 0.001	1.10 ± 0.008
Ethambutol	1.39 ± 0.02	6.52 ± 0.28*	ND	ND	1.49 ± 0.20	8.00 ± 2.71*
Linezolid	1.84 ± 0.17	1.44 ± 0.08	2.54 ± 0.26*	4.43 ± 0.59*	1.87 ± 0.11	1.42 ± 0.05*
Amoxicillin	1.93 ± 0.06	4.33 ± 0.23*	1.58 ± 0.05	3.1 ± 0.18*	2.16 ± 0.17	4.67 ± 0.61*
Rifapentine	1.69 ± 0.12	1.06 ± 0.01	1.49 ± 0.05	1.02 ± 0.005	1.25 ± 0.03	1.0 ± 0.003
Rifampin	13.04 ± 0.34	6.6 ± 0.16*	1.26 ± 0.04	1.14 ± 0.02	4.59 ± 0.28	2.67 ± 0.13*
Amikacin	ND	ND	3.34 ± 0.39*	4.21 ± 0.55*	ND	ND
Kanamycin	ND	ND	1.58 ± 0.001	2.24 ± 0.5	ND	ND
Streptomycin	ND	ND	3.20 ± 0.13*	4.29 ± 0.24*	ND	ND
Roxithromycin	ND	ND	1.10 ± 0.007	1.02 ± 0.002	ND	ND
Clarithromycin	ND	ND	ND	ND	2.5 ± 0.22*	2.52 ± 0.21*
Clofazimine	ND	ND	1.15 ± 0.02	1.0 ± 0.001	1.15 ± 0.01	1.00 ± 0.001

[a] The R values were determined using the inhibition constant, K_i, with the maximum systemic concentration, C_{max} (bound + unbound), of the anti-TB drugs as $[I]$ and the maximum unbound concentration inlet to the liver, $[I]_{u\ inlet,max}$, following the regulatory guidelines described in the text. R values represent means ± SD obtained from the inhibition constants from three or more independent experiments. ND, not determined. *, statistically significant at $P < 0.05$. An asterisk indicates the result is significant according to FDA, MHLW, and EMA guidance for prototypical substrates in which the R values are greater than the corresponding cutoff values recommended by the regulatory authorities under both C_{max} ($R \geq 1.1$, FDA) and $[I]_{u\ inlet,max}$ ($R \geq 1.25$, FDA and MHLW; $R \geq 1.04$, EMA) conditions. The cutoff value is expressed as the suggested value according to the upper limit of the equivalence range by the FDA.

The most significant findings of this study were the high R values of EMB, AMX, and PAS for OATP uptake inhibition (Table 3). EMB is the commonly prescribed first-line anti-TB: thus, the need for further EMB DDI studies is apparent. Similarly PAS, which is used in the treatment of MDR/XDR-TB and other coinfection TB cases, can limit the uptake of coadministered OATP substrates and increase systemic exposure; which leads to altered pharmacokinetic and pharmacodynamic effects. AMX is no longer a common treatment for TB, having been replaced by better therapeutic agents; however, its OATP uptake inhibition effects are still worth noting because caution should be taken using any drugs in regimens involving OATPs in drug disposition. Among the aminoglycosides, streptomycin and amikacin showed high R values for OATP2B1, which could be significant in DDIs with statins, especially atorvastatin and pitavastatin. Furthermore, we evaluated the inhibitory effects of anti-TB drugs on rosuvastatin uptake via OATP1B1 to confirm their inhibitory properties. Rosuvastatin uptake was inhibited significantly by PAS, LZD, EMB, and AMX in HEK-OATP1B1 cells, indicating inhibitory effects of anti-TB drugs on the *in vitro* probe substrates, as well as clinically used substrate drugs (Fig. 4). The R values for PAS, LZD, EMB, and AMX were 55.5, 2.19, 17.9, and 10.0, respectively (Table 4). The R values for rosuvastatin were much higher than those for the probe substrates, indicating a higher probability of DDIs with clinically used OATP substrates, including the statin group. One previous study reported that inhibition of OATP1B1 was associated with rhabdomyolysis caused by cerevastatin; thus, inhibition by anti-TB drugs may contribute to increased statin plasma drug concentrations, which could lead to statin-induced toxicity. A well-known polymorphism in the SLCO1B1 gene (OATP1B1) (c.521T>C/p.V174A, rs4149056) decreases transport activity and markedly increases the concentration of statin-like drugs in plasma, causing adverse reactions. A contribution from OATP2B1 in drug disposition cannot be excluded with regard to transporter-mediated DDIs, especially those drugs transported mainly by this particular transporter. Because of its ubiquitous expression, OATP2B1 may play a role in organs other than the liver and may govern drug uptake in specific microcompartments, such as lung, muscle, or platelets, which control intracellular drug accumulation and potentially alter drug efficacy or toxicity.

To date, many drugs and exogenous compounds have been evaluated as OATP substrates and inhibitors. There are some *in vivo* interactions in which OATP1B1 inhibition can be regarded as an important mechanism. In one study, cyclosporine increased the plasma concentrations of atorvastatin and several other statins, probably partly due to OATP1B1 inhibition (34). In addi-

TABLE 4 The drug-drug interaction index (R value) predicted from *in vitro* OATP1B1-mediated uptake of 1 μM rosuvastatin as inhibited by anti-TB drugs[a]

	Drug-drug interaction index (R value)		
		R value = 1 + $[I]/K_i$	
Anti-TB drug	K_i (μM)	$[I] = C_{max}$	$[I] = [I]_{u\ inlet,max}$
PAS	32.0	27.5 ± 6.8	55.5 ± 12.3*
Rifabutin	12.3	0.05 ± 0.001	1.30 ± 0.31*
Ethambutol	29.8	1.20 ± 0.46	17.9 ± 3.40*
Linezolid	35.0	2.44 ± 0.62	2.19 ± 0.92*
Amoxicillin	13.0	2.56 ± 0.63	10.0 ± 2.4*
Rifapentine	11.0	1.60 ± 0.32	1.16 ± 0.54

[a] The R values were determined using the inhibition constant, K_i, with the maximum systemic concentration, C_{max} (bound + unbound), of the anti-TB drugs as $[I]$ and the maximum unbound concentration inlet to the liver, $[I]_{u\ inlet,max}$, following the guidelines described in the text. The R value represents the mean ± SD from triplicate experiments. An asterisk indicates the result is significant according to FDA, MHLW, and EMA guidance for prototypical substrates in which the R values are greater than the corresponding cutoff values recommended by the regulatory authorities under both C_{max} ($R \geq 1.1$, FDA) and $[I]_{u\ inlet,max}$ ($R \geq 1.25$, FDA and MHLW; $R \geq 1.04$, EMA) conditions. The cutoff value is expressed as the suggested value according to the upper limit of the equivalence range by the FDA.

tion to the statins, cyclosporine has been reported to increase the mean AUC of repaglinide ~2.5-fold in healthy subjects (35). Rifampin is an inhibitor of OATP1B1 and OATP1B3 *in vitro* and also *in vivo*: in a reported case of intravenous administration of rifampin immediately before the "victim" drug, the area under the concentration-time curve (AUC) of atorvastatin increased ~7-fold (29), whereas oral treatment with rifampin over 5 days was reported to decrease the AUC of atorvastatin by ~80%. This was probably due to induction of CYP3A4. These data suggest that hepatic uptake transporters can compensate for reduced uptake by rifampin via OATPs. Also there is a possibility of interaction within the TB regimen; for example, rifampin hepatic uptake can be inhibited by ethambutol, PAS, and other drugs. Moreover, these clinical studies suggest that "victim" drug and inhibitor simultaneous coadministration via the same route can play a key role in drug interactions. In this study, we used the substrates and inhibitor drugs at the same time, incubated with transporter-overexpressing cells, to observe the drug interactions described by others. Furthermore, we conducted this study following FDA guidelines and well-established methods to minimize errors in the design of experimental conditions. We used two experimental models (*Xenopus* oocytes and stable cell lines) to generate more precise and accurate data. Both systems revealed novel inhibitory potential of some anti-TB drugs on OATP uptake with largely similar profiles. Among the anti-TB drugs studied, many *in vitro* and clinical DDI studies on rifampin have been previously reported. However, this study showed that not only rifampin but also other clinically prescribed first- and second-line anti-TB drugs have moderate to significant inhibitory effects on OATP-mediated uptake in the liver. These findings showed a similar pattern to that of a previous report that ethambutol mildly inhibits organic cation transporter (OCT) transporter-mediated uptake and results in DDIs with OCT substrates, such as ^{3}H-labeled 1-methyl-4-phenylpyridinium (MPP) and metformin (36). Anti-TB drug-induced toxicity and/or treatment failure continues to be a serious issue, and DDIs with combination TB-diabetes therapy and anti-HIV therapy have been observed. Such DDIs could be overcome by understanding the involvement of metabolic enzymes and transporters. We believe this study will be helpful to facilitate pharmacotherapy for TB and coinfected disease management. A limitation of this study may be that we evaluated the inhibitory potential and DDI index *R* value for only parent drugs. Some drugs have reactive metabolites with potential inhibitory effects on transporter uptake, which should be taken into consideration in future studies. This *in vitro* study and the DDI index predictions used a static model. Despite the limitations of the static model, it is used widely for DDI prediction because of its simplicity, although it can produce false-negative DDI predictions if precautions are not taken during data fitting. The DDI index *R* score is described in the FDA draft guidance document (27), which only considers a single route of drug disposition. However, clinical DDIs can be impacted by several disposition routes.

In conclusion, to our knowledge, this the first characterization of 22 anti-TB drugs for inhibitory potential against OATP1B1-, OATP2B1-, and OATP1B3-mediated uptake using *Xenopus* oocytes and HEK cell lines. These findings may be helpful to maximize the safety and efficacy of TB pharmacotherapy. To understand this inhibitory interaction potential in greater detail, *in vivo* studies and clinical phenotyping of potential DDIs with anti-TB medications and other concomitantly used classes of drugs are required.

ACKNOWLEDGMENTS

We thank Cho MunJo and Kyung Hun Oh for stable cell line preparation and technical assistance.

We declare no conflicts of interest or other relevant affiliations, financial involvement, or agreement/interest with any organization or governing body. In addition, no outside technical assistance was used in preparing the manuscript.

FUNDING INFORMATION

This work was supported by a National Research Foundation of Korea (NRF) grant funded by the Korea government (MSIP) (grant number R13-2007-023-00000-0) and a grant of Korea Health Technology R&D Project through the Korea Health Industry Development Institute (KHIDI), funded by the Ministry of Health & Welfare, Republic of Korea (grant number HI15C1537).

REFERENCES

1. **Ho RH, Kim RB.** 2005. Transporters and drug therapy: implications for drug disposition and disease. Clin Pharmacol Ther **78:**260–277. http://dx.doi.org/10.1016/j.clpt.2005.05.011.
2. **Shitara Y, Sato H, Sugiyama Y.** 2005. Evaluation of drug-drug interaction in the hepatobiliary and renal transport of drugs. Annu Rev Pharmacol Toxicol **45:**689–723. http://dx.doi.org/10.1146/annurev.pharmtox.44.101802.121444.
3. **Suzuki H, Sugiyama Y.** 2000. Transport of drugs across the hepatic sinusoidal membrane: sinusoidal drug influx and efflux in the liver. Semin Liver Dis **20:**251–263. http://dx.doi.org/10.1055/s-2000-8408.
4. **Kullak-Ublick GA.** 1999. Regulation of organic anion and drug transporters of the sinusoidal membrane. J Hepatol **31:**563–573. http://dx.doi.org/10.1016/S0168-8278(99)80054-3.
5. **Muller M, Jansen PL.** 1997. Molecular aspects of hepatobiliary transport. Am J Physiol **272:**G1285–G1303.
6. **Dean M, Rzhetsky A, Allikmets R.** 2001. The human ATP-binding cassette (ABC) transporter superfamily. Genome Res **11:**1156–1166. http://dx.doi.org/10.1101/gr.GR-1649R.
7. **Fredriksson R, Nordstrom KJ, Stephansson O, Hagglund MG, Schioth HB.** 2008. The solute carrier (SLC) complement of the human genome: phylogenetic classification reveals four major families. FEBS Lett **582:**3811–3816. http://dx.doi.org/10.1016/j.febslet.2008.10.016.
8. **Hagenbuch B.** 2010. Drug uptake systems in liver and kidney: a historic perspective. Clin Pharmacol Ther **87:**39–47. http://dx.doi.org/10.1038/clpt.2009.235.
9. **Collier J, Joekes AM, Philalithis PE, Thompson FD.** 1976. Two cases of ethambutol nephrotoxicity. Br Med J **2:**1105–1106. http://dx.doi.org/10.1136/bmj.2.6044.1105-a,10.1136/bmj.2.6044.1105.
10. **Garcia-Martin F, Mampaso F, de Arriba G, Moldenhauer F, Martin-Escobar E, Saiz F.** 1991. Acute interstitial nephritis induced by ethambutol. Nephron **59:**679–680. http://dx.doi.org/10.1159/000186675.
11. **Shin SS, Hyson AM, Castaneda C, Sanchez E, Alcantara F, Mitnick CD, Fawzi MC, Bayona J, Farmer PE, Kim JY, Furin JJ.** 2003. Peripheral neuropathy associated with treatment for multidrug-resistant tuberculosis. Int J Tuberc Lung Dis **7:**347–353.
12. **Stone WJ, Waldron JA, Dixon JH, Jr, Primm RK, Horn RG.** 1976. Acute diffuse interstitial nephritis related to chemotherapy of tuberculosis. Antimicrob Agents Chemother **10:**164–172. http://dx.doi.org/10.1128/AAC.10.1.164.
13. **Kobayashi Y, Sakai R, Ohshiro N, Ohbayashi M, Kohyama N, Yamamoto T.** 2005. Possible involvement of organic anion transporter 2 on the interaction of theophylline with erythromycin in the human liver. Drug Metab Dispos **33:**619–622. http://dx.doi.org/10.1124/dmd.104.003301.
14. **Bi YA, Kimoto E, Sevidal S, Jones HM, Barton HA, Kempshall S, Whalen KM, Zhang H, Ji C, Fenner KS, El-Kattan AF, Lai Y.** 2012. In vitro evaluation of hepatic transporter-mediated clinical drug-drug interactions: hepatocyte model optimization and retrospective investigation. Drug Metab Dispos **40:**1085–1092. http://dx.doi.org/10.1124/dmd.111.043489.

15. **Tirona RG, Leake BF, Wolkoff AW, Kim RB.** 2003. Human organic anion transporting polypeptide-C (SLC21A6) is a major determinant of rifampin-mediated pregnane X receptor activation. J Pharmacol Exp Ther **304:**223–228. http://dx.doi.org/10.1124/jpet.102.043026.
16. **Vavricka SR, Van Montfoort J, Ha HR, Meier PJ, Fattinger K.** 2002. Interactions of rifamycin SV and rifampicin with organic anion uptake systems of human liver. Hepatology **36:**164–172.
17. **Hirano M, Maeda K, Shitara Y, Sugiyama Y.** 2004. Contribution of OATP2 (OATP1B1) and OATP8 (OATP1B3) to the hepatic uptake of pitavastatin in humans. J Pharmacol Exp Ther **311:**139–146. http://dx.doi.org/10.1124/jpet.104.068056.
18. **Grube M, Kock K, Oswald S, Draber K, Meissner K, Eckel L, Bohm M, Felix SB, Vogelgesang S, Jedlitschky G, Siegmund W, Warzok R, Kroemer HK.** 2006. Organic anion transporting polypeptide 2B1 is a high-affinity transporter for atorvastatin and is expressed in the human heart. Clin Pharmacol Ther **80:**607–620. http://dx.doi.org/10.1016/j.clpt.2006.09.010.
19. **Ho RH, Tirona RG, Leake BF, Glaeser H, Lee W, Lemke CJ, Wang Y, Kim RB.** 2006. Drug and bile acid transporters in rosuvastatin hepatic uptake: function, expression, and pharmacogenetics. Gastroenterology **130:**1793–1806. http://dx.doi.org/10.1053/j.gastro.2006.02.034.
20. **Kopplow K, Letschert K, Konig J, Walter B, Keppler D.** 2005. Human hepatobiliary transport of organic anions analyzed by quadruple-transfected cells. Mol Pharmacol **68:**1031–1038. http://dx.doi.org/10.1124/mol.105.014605.
21. **Vaidyanathan S, Camenisch G, Schuetz H, Reynolds C, Yeh CM, Bizot MN, Dieterich HA, Howard D, Dole WP.** 2008. Pharmacokinetics of the oral direct renin inhibitor aliskiren in combination with digoxin, atorvastatin, and ketoconazole in healthy subjects: the role of P-glycoprotein in the disposition of aliskiren. J Clin Pharmacol **48:**1323–1338. http://dx.doi.org/10.1177/0091270008323258.
22. **Seki S, Kobayashi M, Itagaki S, Hirano T, Iseki K.** 2009. Contribution of organic anion transporting polypeptide OATP2B1 to amiodarone accumulation in lung epithelial cells. Biochim Biophys Acta **1788:**911–917. http://dx.doi.org/10.1016/j.bbamem.2009.03.003.
23. **Satoh H, Yamashita F, Tsujimoto M, Murakami H, Koyabu N, Ohtani H, Sawada Y.** 2005. Citrus juices inhibit the function of human organic anion-transporting polypeptide OATP-B. Drug Metab Dispos **33:**518–523. http://dx.doi.org/10.1124/dmd.104.002337.
24. **Takeda M, Tojo A, Sekine T, Hosoyamada M, Kanai Y, Endou H.** 1999. Role of organic anion transporter 1 (OAT1) in cephaloridine (CER)-induced nephrotoxicity. Kidney Int **56:**2128–2136. http://dx.doi.org/10.1046/j.1523-1755.1999.00789.x.
25. **Amundsen R, Christensen H, Zabihyan B, Asberg A.** 2010. Cyclosporine A, but not tacrolimus, shows relevant inhibition of organic anion-transporting protein 1B1-mediated transport of atorvastatin. Drug Metab Dispos **38:**1499–1504. http://dx.doi.org/10.1124/dmd.110.032268.
26. **Izumi S, Nozaki Y, Maeda K, Komori T, Takenaka O, Kusuhara H, Sugiyama Y.** 2015. Investigation of the impact of substrate selection on in vitro organic anion transporting polypeptide 1B1 inhibition profiles for the prediction of drug-drug interactions. Drug Metab Dispos **43:**235–247. http://dx.doi.org/10.1124/dmd.114.059105.
27. **FDA.** February 2012. Guidance for industry. Drug interaction studies—study design, data analysis, implications for dosing, and labeling recommendations. 2012. FDA, Rockville, MD. http://www.fda.gov/downloads/drugs/guidancecomplianceregulatoryinformation/guidances/ucm292362.pdf.
28. **Ito K, Iwatsubo T, Kanamitsu S, Ueda K, Suzuki H, Sugiyama Y.** 1998. Prediction of pharmacokinetic alterations caused by drug-drug interactions: metabolic interaction in the liver. Pharmacol Rev **50:**387–412.
29. **Lau YY, Huang Y, Frassetto L, Benet LZ.** 2007. Effect of OATP1B transporter inhibition on the pharmacokinetics of atorvastatin in healthy volunteers. Clin Pharmacol Ther **81:**194–204. http://dx.doi.org/10.1038/sj.clpt.6100038.
30. **Lemahieu WP, Hermann M, Asberg A, Verbeke K, Holdaas H, Vanrenterghem Y, Maes BD.** 2005. Combined therapy with atorvastatin and calcineurin inhibitors: no interactions with tacrolimus. Am J Transplant **5:**2236–2243. http://dx.doi.org/10.1111/j.1600-6143.2005.01005.x.
31. **Leonhardt M, Keiser M, Oswald S, Kuhn J, Jia J, Grube M, Kroemer HK, Siegmund W, Weitschies W.** 2010. Hepatic uptake of the magnetic resonance imaging contrast agent Gd-EOB-DTPA: role of human organic anion transporters. Drug Metab Dispos **38:**1024–1028. http://dx.doi.org/10.1124/dmd.110.032862.
32. **Bolhuis MS, van Altena R, van Soolingen D, de Lange WC, Uges DR, van der Werf TS, Kosterink JG, Alffenaar JW.** 2013. Clarithromycin increases linezolid exposure in multidrug-resistant tuberculosis patients. Eur Respir J **42:**1614–1621. http://dx.doi.org/10.1183/09031936.00001913.
33. **Gebhart BC, Barker BC, Markewitz BA.** 2007. Decreased serum linezolid levels in a critically ill patient receiving concomitant linezolid and rifampin. Pharmacotherapy **27:**476–479. http://dx.doi.org/10.1592/phco.27.3.476.
34. **Neuvonen PJ, Niemi M, Backman JT.** 2006. Drug interactions with lipid-lowering drugs: mechanisms and clinical relevance. Clin Pharmacol Ther **80:**565–581. http://dx.doi.org/10.1016/j.clpt.2006.09.003.
35. **Kajosaari LI, Niemi M, Neuvonen M, Laitila J, Neuvonen PJ, Backman JT.** 2005. Cyclosporine markedly raises the plasma concentrations of repaglinide. Clin Pharmacol Ther **78:**388–399. http://dx.doi.org/10.1016/j.clpt.2005.07.005.
36. **Pan X, Wang L, Grundemann D, Sweet DH.** 2013. Interaction of ethambutol with human organic cation transporters of the SLC22 family indicates potential for drug-drug interactions during antituberculosis therapy. Antimicrob Agents Chemother **57:**5053–5059. http://dx.doi.org/10.1128/AAC.01255-13.
37. **Gui C, Miao Y, Thompson L, Wahlgren B, Mock M, Stieger B, Hagenbuch B.** 2008. Effect of pregnane X receptor ligands on transport mediated by human OATP1B1 and OATP1B3. Eur J Pharmacol **584:**57–65. http://dx.doi.org/10.1016/j.ejphar.2008.01.042.
38. **Cui Y, Konig J, Leier I, Buchholz U, Keppler D.** 2001. Hepatic uptake of bilirubin and its conjugates by the human organic anion transporter SLC21A6. J Biol Chem **276:**9626–9630. http://dx.doi.org/10.1074/jbc.M004968200.
39. **Nozawa T, Imai K, Nezu J, Tsuji A, Tamai I.** 2004. Functional characterization of pH-sensitive organic anion transporting polypeptide OATP-B in human. J Pharmacol Exp Ther **308:**438–445.
40. **Noe J, Portmann R, Brun ME, Funk C.** 2007. Substrate-dependent drug-drug interactions between gemfibrozil, fluvastatin and other organic anion-transporting peptide (OATP) substrates on OATP1B1, OATP2B1, and OATP1B3. Drug Metab Dispos **35:**1308–1314. http://dx.doi.org/10.1124/dmd.106.012930.
41. **de Kock L, Sy SK, Rosenkranz B, Diacon AH, Prescott K, Hernandez KR, Yu M, Derendorf H, Donald PR.** 2014. Pharmacokinetics of para-aminosalicylic acid in HIV-uninfected and HIV-coinfected tuberculosis patients receiving antiretroviral therapy, managed for multidrug-resistant and extensively drug-resistant tuberculosis. Antimicrob Agents Chemother **58:**6242–6250. http://dx.doi.org/10.1128/AAC.03073-14.
42. **Way EL, Smith PK, et al.** 1948. The absorption, distribution, excretion and fate of para-aminosalicylic acid. J Pharmacol Exp Ther **93:**368–382.
43. **Tanuma J, Sano K, Teruya K, Watanabe K, Aoki T, Honda H, Yazaki H, Tsukada K, Gatanaga H, Kikuchi Y, Oka S.** 2013. Pharmacokinetics of rifabutin in Japanese HIV-infected patients with or without antiretroviral therapy. PLoS One **8:**e70611. http://dx.doi.org/10.1371/journal.pone.0070611.
44. **Boulanger C, Hollender E, Farrell K, Stambaugh JJ, Maasen D, Ashkin D, Symes S, Espinoza LA, Rivero RO, Graham JJ, Peloquin CA.** 2009. Pharmacokinetic evaluation of rifabutin in combination with lopinavir-ritonavir in patients with HIV infection and active tuberculosis. Clin Infect Dis **49:**1305–1311. http://dx.doi.org/10.1086/606056.
45. **Peloquin CA, Bulpitt AE, Jaresko GS, Jelliffe RW, Childs JM, Nix DE.** 1999. Pharmacokinetics of ethambutol under fasting conditions, with food, and with antacids. Antimicrob Agents Chemother **43:**568–572.
46. **Lee CS, Gambertoglio JG, Brater DC, Benet LZ.** 1977. Kinetics of oral ethambutol in the normal subject. Clin Pharmacol Ther **22:**615–621. http://dx.doi.org/10.1002/cpt1977225part1615.
47. **Dehghanyar P, Burger C, Zeitlinger M, Islinger F, Kovar F, Muller M, Kloft C, Joukhadar C.** 2005. Penetration of linezolid into soft tissues of healthy volunteers after single and multiple doses. Antimicrob Agents Chemother **49:**2367–2371. http://dx.doi.org/10.1128/AAC.49.6.2367-2371.2005.
48. **Franco GC, Baglie S, Ruenis AP, Franco LM, Cogo K, Oshima-Franco Y, Silva P, Groppo FC, Rosalen PL.** 2014. Bioequivalence study of two commercial amoxicillin suspension formulations in healthy human volunteers. Int J Clin Pharmacol Ther **52:**425–430. http://dx.doi.org/10.5414/CP202039.
49. **Pichichero ME, Casey JR, Block SL, Guttendorf R, Flanner H, Markowitz D, Clausen S.** 2008. Pharmacodynamic analysis and clinical trial of

amoxicillin sprinkle administered once daily for 7 days compared to penicillin V potassium administered four times daily for 10 days in the treatment of tonsillopharyngitis due to Streptococcus pyogenes in children. Antimicrob Agents Chemother **52:**2512–2520. http://dx.doi.org/10.1128/AAC.00132-07.

50. **Hafner R, Bethel J, Power M, Landry B, Banach M, Mole L, Standiford HC, Follansbee S, Kumar P, Raasch R, Cohn D, Mushatt D, Drusano G.** 1998. Tolerance and pharmacokinetic interactions of rifabutin and clarithromycin in human immunodeficiency virus-infected volunteers. Antimicrob Agents Chemother **42:**631–639.
51. **Gonzalez D, Schmidt S, Derendorf H.** 2013. Importance of relating efficacy measures to unbound drug concentrations for anti-infective agents. Clin Microbiol Rev **26:**274–288. http://dx.doi.org/10.1128/CMR.00092-12.
52. **Laal S, Mishra RS, Nath I.** 1987. Type 1 reactions in leprosy—heterogeneity in T-cell functions related to the background leprosy type. Int J Lepr Other Mycobact Dis **55:**481–493.
53. **Holdiness MR.** 1989. Clinical pharmacokinetics of clofazimine. A review. Clin Pharmacokinet **16:**74–85. http://dx.doi.org/10.2165/00003088-198916020-00002.
54. **Maeda K, Ikeda Y, Fujita T, Yoshida K, Azuma Y, Haruyama Y, Yamane N, Kumagai Y, Sugiyama Y.** 2011. Identification of the rate-determining process in the hepatic clearance of atorvastatin in a clinical cassette microdosing study. Clin Pharmacol Ther **90:**575–581. http://dx.doi.org/10.1038/clpt.2011.142.
55. **Burman WJ, Gallicano K, Peloquin C.** 2001. Comparative pharmacokinetics and pharmacodynamics of the rifamycin antibacterials. Clin Pharmacokinet **40:**327–341. http://dx.doi.org/10.2165/00003088-200140050-00002.
56. **Tod M, Lortholary O, Seytre D, Semaoun R, Uzzan B, Guillevin L, Casassus P, Petitjean O.** 1998. Population pharmacokinetic study of amikacin administered once or twice daily to febrile, severely neutropenic adults. Antimicrob Agents Chemother **42:**849–856.
57. **Cabana BE, Taggart JG.** 1973. Comparative pharmacokinetics of BB-K8 and kanamycin in dogs and humans. Antimicrob Agents Chemother **3:**478–483. http://dx.doi.org/10.1128/AAC.3.4.478.
58. **Gordon RC, Regamey C, Kirby WM.** 1972. Serum protein binding of the aminoglycoside antibiotics. Antimicrob Agents Chemother **2:**214–216. http://dx.doi.org/10.1128/AAC.2.3.214.
59. **Zhu M, Burman WJ, Jaresko GS, Berning SE, Jelliffe RW, Peloquin CA.** 2001. Population pharmacokinetics of intravenous and intramuscular streptomycin in patients with tuberculosis. Pharmacotherapy **21:**1037–1045. http://dx.doi.org/10.1592/phco.21.13.1037.34625.
60. **Puri SK, Lassman HB.** 1987. Roxithromycin: a pharmacokinetic review of a macrolide. J Antimicrob Chemother **20**(Suppl B)**:**89–100. http://dx.doi.org/10.1093/jac/20.suppl_B.89.
61. **Andrews JM, Ashby JP, Wise R.** 1987. Factors affecting the in-vitro activity of roxithromycin. J Antimicrob Chemother **20**(Suppl B)**:**31–37. http://dx.doi.org/10.1093/jac/20.suppl_B.31.
62. **Egelund EF, Weiner M, Singh RP, Prihoda TJ, Gelfond JA, Derendorf H, MacKenzie WR, Peloquin CA.** 2014. Protein binding of rifapentine and its 25-desacetyl metabolite in patients with pulmonary tuberculosis. Antimicrob Agents Chemother **58:**4904–4910. http://dx.doi.org/10.1128/AAC.01730-13.